

## Metal–Organic Framework Assembled from T-Shaped and Octahedral Nodes: A Mixed-Linker Strategy To Create a Rare Anatase TiO<sub>2</sub> Topology

Jennifer M. Verduzco,<sup>†</sup> Haemi Chung,<sup>†</sup> Chunhua Hu,<sup>§</sup> and Wonyoung Choe<sup>\*†‡</sup>

<sup>†</sup>Department of Chemistry and <sup>‡</sup>Nebraska Center for Materials and Nanoscience, University of Nebraska-Lincoln, Lincoln, Nebraska 68588-0304, and <sup>§</sup>Department of Chemistry, New York University, New York, New York 10003-6688

Received May 20, 2009

A novel porphyrin paddlewheel framework (PPF-25), assembled from a zinc paddlewheel cluster and mixed linkers (4,4'-bipyridyl; zinc 5,15-di(4-carboxyphenyl)-10,20-diphenylporphyrin), has been synthesized and structurally characterized. T-shaped organometallic nodes are generated, and the resulting structure is closely related to anatase, a polymorph of TiO<sub>2</sub>.

The recent exponential growth in the synthesis and characterization of a new class of inorganic–organic hybrid materials, often referred to as metal–organic frameworks (MOFs), has been driven, in part, by their fascinating topologies and possible applications, ranging from gas storage to heterogeneous catalysts.<sup>1–3</sup> These MOFs are self-assembled from two different types of structural components (organic and inorganic nodes) and commonly form a 3D net topology found in solid-state materials.<sup>3,4</sup> Among the many 3D nets identified in MOFs,<sup>4</sup> framework structures with heteronodal nets are of particular interest.<sup>4,5</sup> Examples include various (3,6) nets, such as rutile (**rtl**), anatase (**ant**), **qom**,

and **pyr**, assembled from 3-connected organic linkers and 6-connected inorganic building blocks.<sup>6–11</sup>

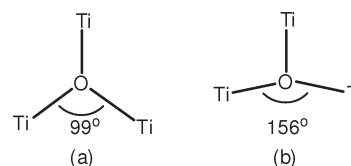


**Figure 1.** Coordination geometry around oxygen in (a) rutile and (b) anatase shown with  $2\theta$  (Ti–O–Ti) values of  $99^\circ$  and  $156^\circ$ , respectively.

Of these (3,6) nets, **rtl** and **ant** are polymorphs of TiO<sub>2</sub>.<sup>12,13</sup> A notable structural difference between the **rtl** and **ant** architectures can be traced to the coordination geometry of the 3-connected oxygen atom.<sup>12</sup> The geometries around the oxygen atom in **rtl** and **ant** are planar Y and T shapes, respectively (see Figure 1).<sup>12</sup> In both cases, Ti atoms are surrounded by six O atoms, forming an octahedral geometry.<sup>12</sup> To achieve these net topologies in MOFs, tritopic Y-shaped organic linkers are frequently used; the most notable example is 1,3,5-benzenetricarboxylic acid (BTB).<sup>7–9</sup> In

\*To whom correspondence should be addressed. E-mail: choe2@unlnotes.unl.edu. Phone: +1-402-472-0751. Fax: +1-402-472-7860.

(1) (a) Rowsell, J. L. C.; Yaghi, O. M. *Angew. Chem., Int. Ed.* **2005**, *44*, 4670. (b) Dincă, M.; Long, J. R. *Angew. Chem., Int. Ed.* **2008**, *47*, 6766. (c) Férey, G.; Mellot-Draznieks, C.; Serre, C.; Millange, F.; Dutour, J.; Surblé, S.; Margiolaki, I. *Science* **2005**, *309*, 2040. (d) Long, J. R.; Yaghi, O. M. *Chem. Soc. Rev.* **2009**, *38*, 1213.

(2) (a) Cho, S.-H.; Ma, B.; Nguyen, S. T.; Hupp, J. T.; Albrecht-Schmitt, T. E. *Chem. Commun.* **2006**, 2563. (b) Seo, J. S.; Whang, D.; Lee, H.; Jun, S. I.; Oh, J.; Jeon, Y. J.; Kim, K. *Nature* **2000**, *404*, 982. (c) Kitagawa, S.; Kitaura, R.; Noro, S. *Angew. Chem., Int. Ed.* **2004**, *43*, 2334.

(3) O'Keeffe, M.; Eddaoudi, M.; Li, H.; Reineke, T.; Yaghi, O. M. *J. Solid State Chem.* **2000**, *152*, 3.

(4) Öhrström, L.; Larsson, K. *Molecule Based Materials, The Structural Network Approach*; Elsevier: Amsterdam, The Netherlands, 2005.

(5) Examples of network structures with multiple nodes are (3,6), (4,6), and (4,8) nets. See: (a) Chun, H.; Kim, D.; Dybtsev, D. N.; Kim, K. *Angew. Chem., Int. Ed.* **2004**, *43*, 971. (b) Natarajan, R.; Savitha, G.; Dominiak, P.; Wozniak, K.; Moorthy, J. N. *Angew. Chem., Int. Ed.* **2005**, *44*, 2115. (c) Du, M.; Zhang, Z.-H.; Zhao, X.-J.; Xu, Q. *Inorg. Chem.* **2006**, *45*, 5785. (d) Lan, Y.-Q.; Li, S.-L.; Li, Y.-G.; Su, Z.-M.; Shao, K.-Z.; Wang, X.-L. *CrystEngComm* **2008**, *10*, 1129.

(6) For the three-letter net classification, see: O'Keeffe, M.; Peskov, M. M.; Ramsden, S. J.; Yaghi, O. M. *Acc. Chem. Res.* **2008**, *41*, 1782.

(7) For the **rtl** net, see: (a) Xie, L. H.; Liu, S. X.; Gao, B.; Zhang, C. D.; Sun, C. Y.; Li, D. H.; Su, Z. M. *Chem. Commun.* **2005**, 2402. (b) Zhao, X.; Zhu, G.; Fang, Q.; Wang, Y.; Sun, F.; Qiu, S. *Cryst. Growth Des.* **2009**, *9*, 737.

(8) For the **ant** net, see: (a) Caskey, S. R.; Wong-Foy, A. G.; Matzger, A. J. *Inorg. Chem.* **2008**, *47*, 7751. (b) Xiang, S.; Wu, X.; Zhang, J.; Fu, R.; Hu, S.; Zhang, X. *J. Am. Chem. Soc.* **2005**, *127*, 16352.

(9) For the **qom** net, see: Chae, H. K.; Siberio-Perez, D. Y.; Kim, J.; Go, Y. B.; Eddaoudi, M.; Matzger, A. J.; O'Keeffe, M.; Yaghi, O. M. *Nature* **2004**, *427*, 523.

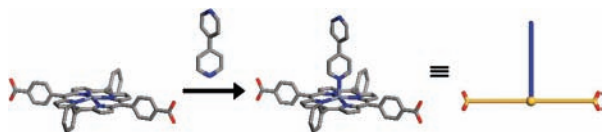
(10) For the **pyr** net, see: Chae, H. K.; Kim, J.; Friedrichs, O. D.; O'Keeffe, M.; Yaghi, O. M. *Angew. Chem., Int. Ed.* **2003**, *42*, 3907.

(11) (a) Delgado-Friedrichs, O.; O'Keeffe, M.; Yaghi, O. M. *Acta Crystallogr., Sect. A* **2003**, *59*, 22. (b) For other (3,6) nets, see: Du, M.; Zhang, Z.-H.; Tang, L.-F.; Wang, X.-G.; Zhang, X.-J.; Batten, S. R. *Chem. Eur. J.* **2007**, *13*, 2578.

(12) (a) Cromer, D. T.; Herrington, K. *J. Am. Chem. Soc.* **1955**, *77*, 4708. (b) Meagher, E. P.; Lager, G. A. *Can. Mineral.* **1979**, *17*, 77. (c) Horn, M.; Scherdtfeger, C. F.; Meagher, E. P. *Z. Kristallogr.* **1972**, *136*, 273. (d) Burdett, J. K.; Hughbanks, T.; Miller, G. J.; Richardson, J. W.; Smith, J. V. *J. Am. Chem. Soc.* **1987**, *109*, 3639. (e) O'Keeffe, M. *Acta Crystallogr., Sect. A* **1977**, *33*, 924. (f) Burdett, J. K. *Inorg. Chem.* **1985**, *24*, 2244.

(13) Another polymorph of TiO<sub>2</sub> is brookite (**brk**). However, this topology has not been observed in MOFs.<sup>5</sup>

**Scheme 1.** Schematic Representation of the Formation of a T-Shaped Organometallic Node Using *trans*-ZnDCPP and bpy



contrast, T-shaped organic linkers are seldom used in MOF synthesis,<sup>14</sup> possibly because of the difficulties encountered in the design and synthesis of such exotic ligands.<sup>14c</sup>

We previously reported a MOF called PPF-6 (PPF = porphyrin paddlewheel framework) with a (3,6)-connected, 2D CdI<sub>2</sub> topology using 5,10-di(4-carboxyphenyl)-15,20-diphenylporphyrin (*cis*-DCPP) and 4,4'-bipyridyl (bpy).<sup>15,16</sup> In this CdI<sub>2</sub> topology, *cis*-ZnDCPP and bpy form an extraordinary trigonal-pyramidal metalloligand node.

In this Communication, we use a different porphyrin ligand, 5,15-di(4-carboxyphenyl)-10,20-diphenylporphyrin (*trans*-DCPP) and bpy and create a new T-shaped metalloligand node (Scheme 1). Combined with an octahedral Zn<sub>2</sub>(COO)<sub>4</sub> SBU, the resulting net is a rare example of a (3,6) **ant** topology. Such a mixed-linker approach is useful in creating a node geometry that is not easily accessible to MOF chemists.<sup>17</sup>

The title compound, PPF-25, was synthesized by a solvothermal reaction of zinc nitrate hexahydrate (5.8 mg, 0.02 mmol), *trans*-DCPP (7.0 mg, 0.01 mmol), and bpy (2.3 mg, 0.015 mmol) in a mixture of *N,N*-dimethylformamide (DMF) and ethanol [2.0 mL, 3:1 (v/v)]. The mixture was sealed in a small capped vial and sonicated for 30 s to ensure homogeneity. The vial then was heated at 80 °C in an oven for 24 h, followed by slow cooling to room temperature for 9 h, yielding square purple crystals. The structure of PPF-25 was determined by single-crystal X-ray diffraction (XRD),<sup>18</sup> and its purity was confirmed by elemental analysis and powder XRD (see Figure S1 in the Supporting Information).<sup>19</sup>

The PPF-25 structure can be explained in the following manner. The structure is based on 2D porphyrin sheets (Figure 2a) assembled from *trans*-DCPP linkers and dinuclear Zn<sub>2</sub>(COO)<sub>4</sub> paddlewheel secondary building units (SBUs) at a ratio of 2:1. Here, dinuclear paddlewheel Zn atoms are connected by four *trans*-ZnDCPP, forming a 2D square (4,4) grid pattern. This ratio is different from the 1:1 ratio found in other tetratopic porphyrin-based MOFs and can be compared with PPF-1 (Figure 2b).<sup>20</sup> Therefore,

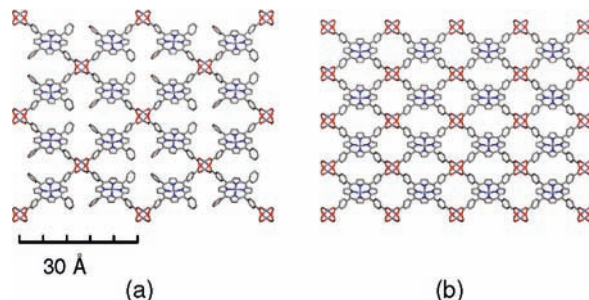


**Figure 2.** 2D porphyrinic (4,4) grids assembled from (a) *trans*-DCPP (PPF-25) and (b) TCPP [TCPP = 5,10,15,20-tetrakis(4-carboxyl)-21H,23H-porphine, PPF-1]<sup>20</sup> linkers.

the 2D pattern of PPF-25 can be considered a “defective-paddlewheel” structure of PPF-1. As shown in Figure 2, PPF-25 is an open-framework structure. The distance between the nearest paddlewheels is 23.6 Å, and the diagonal distances are 31.9 and 34.8 Å, slightly distorted from the regular square grid pattern. The framework density calculated from single-crystal XRD data is 0.45 cm<sup>3</sup>/g, with a solvent-accessible volume of 42,738 Å<sup>3</sup> (72% of the unit cell volume in PPF-25), based on a PLATON calculation. However, PPF-25 is unstable upon evacuation at 100 °C.

The 2D sheet of PPF-25 is further coordinated by bpy linkers. One of the pyridyl ends of bpy binds to the Zn center in the porphyrin core. The overall geometry of this metalloligand node becomes T-shaped because of the strong preference of the Zn atom inside the porphyrin to be five-coordinated.<sup>21</sup> The bpy–ZnDCPP interaction shows a Zn–N interaction of 2.148 Å, consistent with that of other five-coordinated zinc porphyrins.<sup>21</sup> This T-shaped organometallic node offers two carboxylate groups and one pyridyl group to the zinc paddlewheel SBU. In contrast, the zinc paddlewheel SBU can accept four carboxylate and two pyridyl groups. Therefore, the ratio of T-shaped nodes to zinc paddlewheel SBUs in the PPF-25 structure is 2:1. The pyridyl group in this T-shaped node binds to the axial coordination site in the zinc paddlewheel, while the carboxylate sites are connected to equatorial zinc paddlewheels. The resulting structure is a noninterpenetrating **ant** topology (Figure 3).<sup>8</sup> 1D ladders formed from the T-shaped nodes and octahedral paddlewheel nodes are evident in Figure 3. These 1D ladders are stacked in an *ABCD* fashion (Figure S2 in the Supporting Information). Such ladder motifs are commonly found in MOFs.<sup>14</sup>

Compared with other (3,6)-coordinated nets, **ant** is a rare topology in MOFs: to the best of our knowledge, only two other structures have been reported in the literature.<sup>8</sup> A noteworthy example with **ant** topology is the Zn/BTB **ant** compound, assembled from trigonal Y-shaped linkers (BTB).<sup>8</sup> To adopt the **ant** topology, the Zn<sub>4</sub>O octahedral node in this compound is severely distorted to link trigonal BTB linkers.<sup>22</sup>

(14) For the use of T-shaped nodes in MOFs, see: (a) Zaworotko, M. J. *Chem. Commun.* **2001**, 1. (b) Suh, M. P.; Cheon, Y. E.; Lee, E. Y. *Coord. Chem. Rev.* **2008**, 252, 1007. (c) Yong, G.; Qiao, S.; Xie, Y.; Wang, Z. *Eur. J. Inorg. Chem.* **2006**, 4483.

(15) Choi, E.-Y.; Barron, P. M.; Novotny, R. W.; Hu, C.; Kwon, Y.-U.; Choe, W. *CrystEngComm* **2008**, 10, 824.

(16) For reviews on porphyrin-based coordination polymers, see: (a) DeVries, L. D.; Choe, W. *J. Chem. Crystallogr.* **2009**, 39, 229. (b) Goldberg, I. *CrystEngComm* **2008**, 10, 637. (c) Suslick, K. S.; Bhyrappa, P.; Chou, J.-H.; Kosal, M. E.; Nakagaki, S.; Smithenry, D. W.; Wilson, S. *Acc. Chem. Res.* **2005**, 38, 283.

(17) (a) Stork, J. R.; Thoi, V. S.; Cohen, S. M. *Inorg. Chem.* **2007**, 46, 11213. (b) Halper, S. R.; Do, L.; Stork, J. R.; Cohen, S. M. *J. Am. Chem. Soc.* **2006**, 128, 15255.

(18) Crystallographic data: C<sub>112</sub>H<sub>68</sub>N<sub>12</sub>O<sub>8</sub>Zn<sub>4</sub>, orthorhombic, *Fddd*, *a* = 31.8557(19) Å, *b* = 34.817(2) Å, *c* = 52.617(3) Å, *V* = 58359(6) Å<sup>3</sup>, *Z* = 8, ρ<sub>calcd</sub> = 0.449 g cm<sup>-3</sup>, R1 = 0.0408, wR2 = 0.0901 [*I* > 2σ(*I*), after SQUEEZE].

(19) Elem. anal. Calcd for PPF-25, [Zn(*trans*-ZnDCPP)(bpy)]·DMF·1.7H<sub>2</sub>O: C, 65.04; H, 4.11; N, 9.00. Found: C, 65.13; H, 4.03; N, 9.00.

(20) Choi, E.-Y.; Wray, C. A.; Hu, C.; Choe, W. *CrystEngComm* **2009**, 11, 553.

(21) (a) Choi, E.-Y.; Barron, P. M.; Novotny, R. W.; Son, H.-T.; Hu, C.; Choe, W. *Inorg. Chem.* **2009**, 48, 426. (b) Chung, H.; Barron, P. M.; Novotny, R. W.; Son, H.-T.; Hu, C.; Choe, W. *Cryst. Growth Des.* **2009**, 9, 3327.

(22) (a) The octahedral angles (corresponding to O–Ti–O angles in anatase) found in this Zn/BTB **ant** compound are 68–70° and 110–113°, representing a significant deviation from the ideal octahedral angle of 90° (see also Figure S5 in the Supporting Information). (b) The stability of **rtl** and **ant** is closely related to the angular distortion of Ti–O–Ti. See refs 12d, 12f, and 22c. (c) Fahmi, A.; Minot, C.; Silvi, B.; Causá, M. *Phys. Rev. B* **1993**, 47, 11717.

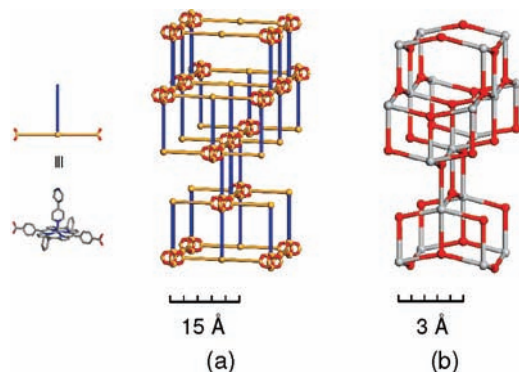


**Figure 3.** Crystal structures of (a) PPF-25 and (b) its parent topology anatase (**ant**), showing the isostructural relationship.

As exemplified by this case and PPF-25, the **ant** topology can accept both Y- and T-shaped nodes.

In contrast, another (3,6) topology, **rtl**, is not flexible regarding the choice of trigonal nodes. To illustrate this, the distances ( $l$ ) between trigonal nodes are estimated as  $2d \sin(\theta/2)$  and  $2d \cos \theta$ , in **ant** and **rtl** topologies, respectively (where  $d$  is the distance between trigonal and octahedral nodes and  $2\theta$  is the angle of the trigonal node).<sup>22c</sup> When the trigonal node becomes T-shaped ( $2\theta = 180^\circ$ ) in an ideal **rtl** topology, the distance between the adjacent trigonal nodes becomes zero, suggesting that the construction of an **rtl** topology using T-shaped nodes becomes unfavorable because of such steric effect (see Chart 1).<sup>23</sup> In PPF-25, the **ant** topology is favored. The competing **rtl** topology cannot accommodate a T-shaped linker, which suggests that the shape of the trigonal linker plays an important role in the framework assembly of (3,6) nets.<sup>24</sup>

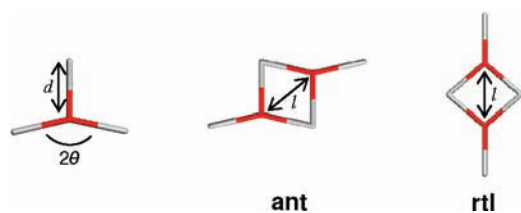
T-shaped nodes, and their use in MOF design, have been of interest in recent decades.<sup>14,25</sup> More than 30 years ago, Wells noted that framework architectures can be built using T-shaped nodes to form extraordinary architectures such as brick wall, herringbone, bilayer, and basket weave.<sup>25a</sup>

(23) A similar trend can be seen in uninodal 3-connected nets. For example, the **srs** net demands an equilateral triangle node, but the **ths** net can adopt Y- or T-shaped nodes. See: Yaghi, O. M.; O'Keeffe, M.; Ockwig, N. W.; Chae, H. K.; Eddaoudi, M.; Kim, J. *Nature* **2003**, *423*, 705.

(24) It is interesting to compare the cell volumes of the two topologies, **rtl** and **ant**. The cell volumes can be estimated as  $16d^3(1 + \cos \theta) \sin^2 \theta$  and  $8d^3(1 + \cos \theta)^2 \sin \theta$  for the **ant** and **rtl** topologies, respectively. As shown in Figure S6 in the Supporting Information, the **ant** topology is less dense than the **rtl** topology in the range of  $106.3^\circ < 2\theta < 180^\circ$ .

(25) (a) Wells, A. F. *Three Dimensional Nets and Polyhedra*; Wiley: New York, 1977. (b) Ienco, A.; Proserpio, D. M.; Hoffmann, R. *Inorg. Chem.* **2004**, *43*, 2526.

**Chart 1**



The T-shaped nodes previously established in MOFs are mainly metallic nodes.<sup>14</sup> Utilizing a new type of organometallic node composed of mixed linkers could represent an important strategy in uncovering a variety of uninodal or heteronodal net patterns that have been predicted theoretically but are difficult to achieve experimentally. A detailed analysis of the binding mode and symmetry of nodes is a key component of achieving rare topologies in MOFs.<sup>23,26</sup>

Finally, we compare two topologies: the **ant** topology found in the title compound PPF-25 assembled from *trans*-DCPP and the  $\text{CdI}_2$  topology constructed from *cis*-DCPP reported previously in PPF-6.<sup>15</sup> The 3-connected organometallic nodes form either cubic closest-packing (**ant**) or hexagonal closest-packing ( $\text{CdI}_2$ ) lattices, and the octahedral nodes are distributed in a zig-zag pattern (**ant**) or in alternating 2D sheets ( $\text{CdI}_2$ ).<sup>12d,15</sup> In both cases, a mixed-linker synthetic strategy has been proven to be useful in yielding extremely rare topologies in MOFs.<sup>27</sup> We are currently investigating the photoluminescence properties of PPF-25.

In summary, we have demonstrated that a porphyrin linker can be used to create T-shaped nodes composed of mixed linkers, thereby forming a rare anatase (**ant**) topology.

**Acknowledgment.** The authors acknowledge financial support from Nebraska EPSCoR, the Nebraska Center for Energy Sciences Research, the Nebraska Center for Materials and Nanoscience, and the Research Council of the University of Nebraska-Lincoln.

**Supporting Information Available:** Crystallographic data in CIF format, powder XRD pattern, TGA data, additional figures, and a table listing  $\text{TiO}_2$  topologies. This material is available free of charge via the Internet at <http://pubs.acs.org>.

(26) (a) For example, various zeolite-like MOFs have been synthesized by mimicking the O–Si–O angle ( $144^\circ$ ). See: Park, K. S.; Ni, Z.; Côté, A. P.; Choi, J. Y.; Huang, R.; Uribe-Romo, F. J.; Chae, H. K.; O'Keeffe, M.; Yaghi, O. M. *Proc. Natl. Acad. Sci. U.S.A.* **2006**, *103*, 10186. See also: (b) Yaghi, O. M.; O'Keeffe, M. *Chem. Eur. J.* **1999**, *5*, 2796.

(27)  $\text{CdI}_2$  topology is also a rare topology in MOFs. See ref 15.